

Article

Impulse Wave Runup on Steep to Vertical Slopes

Frederic M. Evers ^{*}  and Robert M. Boes 

Laboratory of Hydraulics, Hydrology and Glaciology (VAW), ETH Zurich, CH-8093 Zürich, Switzerland; boes@vaw.baug.ethz.ch

* Correspondence: evers@vaw.baug.ethz.ch; Tel.: +41-44-633-0877

Received: 9 November 2018; Accepted: 18 December 2018; Published: 7 January 2019



Abstract: Impulse waves are generated by landslides or avalanches impacting oceans, lakes or reservoirs, for example. Non-breaking impulse wave runup on slope angles ranging from 10° to 90° (V/H : 1/5.7 to 1/0) is investigated. The prediction of runup heights induced by these waves is an important parameter for hazard assessment and mitigation. An experimental dataset containing 359 runup heights by impulse and solitary waves is compiled from several published sources. Existing equations, both empirical and analytical, are then applied to this dataset to assess their prediction quality on an extended parameter range. Based on this analysis, a new prediction equation is proposed. The main findings are: (1) solitary waves are a suitable proxy for modelling impulse wave runup; (2) commonly applied equations from the literature may underestimate the runup height of small wave amplitudes; (3) the proposed semi-empirical equations predict the overall dataset within $\pm 20\%$ scatter for relative wave crest amplitudes ϵ , i.e., the wave crest amplitude normalised with the stillwater depth, between 0.007 and 0.69.

Keywords: impulse wave; solitary wave; landslide tsunami; wave runup; runup prediction

1. Introduction

Impulse waves are generated by very rapid gravity-driven mass movements including landslides and avalanches impacting a body of water (Heller et al. [1]). The slide energy is transferred to the water column and a wave train is generated, which propagates away from the impact location. Especially water bodies with steep shorelines, e.g., fjords, mountain lakes or reservoirs, are prone to this tsunami-like hazard. Roberts et al. [2] compiled a global catalogue with 254 landslide-generated impulse wave events. In the past, extreme absolute impulse wave runup heights were observed in Lituya Bay, USA, in 1958 with 524 m (Miller [3]), Chehalis Lake, Canada, in 2007 with 38 m (Roberts et al. [4]), and Taan Fjord, USA, in 2015 with 193 m (Higman et al. [5]).

For hazard mitigation, the runup height R is of primary interest (Figure 1). While the impulse wave events given above are extreme cases, comparably small runup heights at densely populated lake shores may already cause substantial damage (Fuchs and Boes [6]). Particularly in reservoirs, where there is a freeboard of just a few meters between the stillwater level and the dam crest, the prediction of runup by small impulse wave amplitudes needs to be as accurate as possible to prevent overtopping. Müller [7] conducted experiments specifically designed to study the runup of impulse waves and derived an empirical prediction equation for the runup height induced by the first or leading wave, respectively, of the impulse wave train. However, also equations derived from experiments with solitary waves are commonly applied to predict runup heights by impulse waves (e.g., Bregoli et al. [8], McFall and Fritz [9]). While a solitary wave features a single wave crest, impulse waves are characterized by an outgoing wave train with multiple wave crests and troughs (Figure 1).

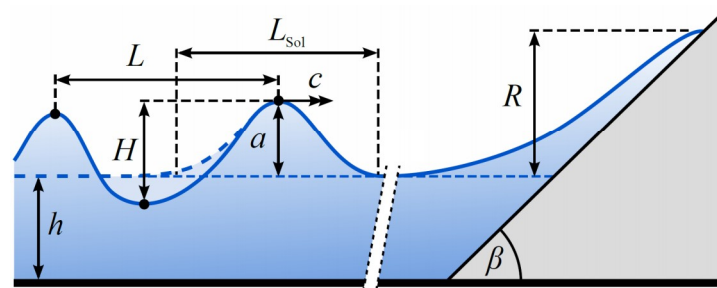


Figure 1. Definition plot for impulse (solid line) and solitary wave (dashed line) runup on an inclined slope.

This study focuses on non-breaking impulse wave runup on steep slopes, i.e., slope angles $\beta \geq 10^\circ$ (Figure 1). First, runup equations from the literature are discussed. Since there is a multitude of studies on solitary wave runup on gentle slopes (Pujara et al. [10], Hafsteinnsson et al. [11]), only equations derived from experiments with $\beta \geq 10^\circ$ or those commonly applied for this parameter range are included. A dataset consisting of measured runup heights from both impulse wave and solitary wave (index Sol) runup experiments with β between 10° and 90° (vertical wall) is then compiled from published experimental data. Subsequently, the runup equations are applied to these data for runup prediction. Based on this comparison, a semi-empirical runup equation is proposed. The discussion includes the limitations of this equation and assesses the significance of scale effects.

2. Runup Equations

The governing parameters included in the prediction equations for the runup height described below are: wave crest amplitude a , wave height H , wave length L , stillwater depth h , and runup slope angle β (Figure 1). While H is a combined parameter of the first wave crest and trough amplitudes for impulse waves, $H = a$ for solitary waves. The relative wave crest amplitude is defined as $\varepsilon = a / h$. While the length of a solitary wave is infinite (Dean and Dalrymple [12]), it may be approximated with L_{Sol} as the effective wave length (Lo et al. [13]). For empirically derived prediction equations included below, the corresponding datasets are described in the following section.

Müller [7] approximated the runup height R of impulse waves based on wave channel experiments with

$$\frac{R}{h} = 1.25 \left(\frac{H}{h} \right)^{1.25} \left(\frac{H}{L} \right)^{-0.15} \left(\frac{90^\circ}{\beta} \right)^{0.2} \quad (1)$$

Equation (1) contains the two governing wave parameters, H and L . The last term including β equals to 1 for 90° and increases for decreasing β . To predict the runup height of a solitary wave, its effective wave length may be approximated with (Lo et al. [13])

$$L_{Sol} = \frac{2\pi h}{\sqrt{0.75\varepsilon}} \quad (2)$$

Hall and Watts [14] approximated the runup height R of solitary waves also based on wave channel experiments with

$$\frac{R}{h} = 3.05 \left(\frac{\beta}{180^\circ} \pi \right)^{-0.13} \varepsilon^{1.15 \left(\frac{\beta}{180^\circ} \pi \right)^{0.02}} \quad (3)$$

In the original publication, the runup slope angle β was expressed in radians, whereas its unit is in ($^\circ$) in Equation (3). Since this equation was derived for solitary wave runup, ε is included as the single governing wave parameter. Hall and Watts [14] state the application range for Equation (3) with β between 12° and 45° . A different equation is given for β between 5° and 12° . However, the latter will not be considered in the further analysis, while Equation (3) will be applied to runup angles between 10° and 45° for simplification.

As the third empirical runup equation, Fuchs and Hager [15] approximated the runup height R of solitary waves in wave channel experiments with

$$\frac{R}{h} = 3(\tan \beta)^{-0.05} \varepsilon \quad (4)$$

The governing wave parameter is ε . The runup slope β is included in a tangent function. As the tangent of $\beta = 90^\circ$ is not defined, wave runup at a vertical wall may not be predicted with Equation (4).

Synolakis [16] developed an approximate solution of the nonlinear wave theory and applied it to derive an equation describing the maximum runup height R of a solitary wave with

$$\frac{R}{h} = 2.831(\cot \beta)^{0.5} \varepsilon^{1.25}, \quad (5)$$

referred to as *the runup law*. Equation (5) is formally correct for $\varepsilon^{0.5} \gg 0.288 \tan \beta$ (Synolakis [16]). The theoretical approach is compared to own experimental data for a gentle slope with $\beta \approx 2.9^\circ$ ($\tan \beta = 1/19.85$) as well as to selected experiments with non-breaking wave runup data by Hall and Watts [14] with β between 5° and 45° . Synolakis [16] finds a satisfactory agreement except for $\beta = 45^\circ$. Similar to Equation (4), the cotangent of $\beta = 90^\circ$ equals to zero and therefore wave runup at a vertical wall may not be predicted with Equation (5).

Except for Equation (1), none of the other equations considered runup at a vertical wall, i.e., $\beta = 90^\circ$. Su and Mirie [17] studied the collision of two solitary waves and conducted a perturbation analysis of this phenomenon to the third order. If viscosity and surface tension effects are neglected, the case of two colliding solitary waves with the same amplitude is equal to the runup of a single wave at a vertical wall (Cooker et al. [18]). The maximum runup height R for $\beta = 90^\circ$ is stated by Su and Mirie [17] with

$$\frac{R}{h} = 2\varepsilon + \frac{1}{2}\varepsilon^2 + \frac{3}{4}\varepsilon^3. \quad (6)$$

For very small relative wave amplitudes, the relative runup height R/h converges to 2ε . Maxworthy [19] presents experimental results for both wave-wave interaction and wave-wall interaction, which indicate that the maximum superposed wave amplitude or runup height, respectively, is approximately 10% higher in the former than in the latter case. However, these experiments were conducted at stillwater depths between 4.5 and 6.7 cm and viscosity as well as surface tension effects might have had a more significant influence compared to larger scales.

3. Datasets

Five experimental datasets were included in the analysis presented herein: Müller [7] ($n = 166$), Hall and Watts [14] ($n = 138$), Fuchs [20] ($n = 19$), Street and Camfield [21] ($n = 22$), and Maxworthy [19] ($n = 14$) with a total of $n = 359$ experiments. Their respective key parameter ranges are summarized in Table 1. In Müller's [7] experiments, wave trains with multiple wave crests and troughs were generated to reproduce landslide generated impulse wave characteristics, while the other experimental series document solitary waves, i.e., $a = H$ (Figure 1). Therefore, the waves generated in the experiments by Müller [7] will be referred to in the following as *impulse waves*, while the remaining are *solitary waves*. The generated relative wave amplitudes ε range from 0.007 to 0.69 and runup slope angles β from 10° to 90° (vertical wall). While empirical prediction equations were directly derived from the datasets by Müller [7], Hall and Watts [14], and Fuchs [15] as described in the previous section, the data by Street and Camfield [20] and Maxworthy [19] for $\beta = 90^\circ$ is included to assess the analytically derived Equation (6) by Su and Mirie [17].

Table 1. Parameter ranges of datasets included in the analysis.

Dataset	h (m)	β (°)	ϵ (-)	R/h (-)	a/H (-)
Müller [7]	0.2–0.6	18.4–90	0.007–0.495	0.014–1.143	0.57–1.04
Hall and Watts [14]	0.15–0.69	10–45	0.05–0.56	0.09–1.82	1 ⁽¹⁾
Fuchs [20]	0.2	11.3–33.7	0.10–0.69	0.33–2.30	1 ⁽¹⁾
Street and Camfield [21]	0.152–0.305	90	0.10–0.65	0.18–1.75	1 ⁽¹⁾
Maxworthy [19]	0.045–0.067	90	0.12–0.67	0.28–1.55	1 ⁽¹⁾

⁽¹⁾ Solitary wave.

Müller [7] conducted experiments in a wave channel with a length of 19.25 m, a width of 1 m, and a depth of 1.2 m. The impulse waves were generated by a rectangular box falling vertically onto the water surface at one end of the channel. The box mass ranged from 118 to 422 kg. By adjusting box mass, drop height, and water depth, tests with differing wave characteristics were achieved. Parallel wire wave gauges were applied for measuring the water surface displacement. The installed slope angles β were 18.4°, 45° and 90°. For tracking the maximum runup height R of the first wave at the vertical wall ($\beta = 90^\circ$), also wire wave gauges were applied. For the two milder slopes, R was optically recorded. The accuracy of the wave gauges is given with ± 0.1 mm and for the optical method with ± 1 to 2 mm. Repeatability tests yielded deviation $< 1\%$ for runup heights $R > 40$ mm and a larger scatter of 10% for $R < 40$ mm. Figure 2 shows the wave crest celerities c (see Figure 1) of the first outgoing wave within the impulse wave train as a function of ϵ . Compared to the celerity of a solitary wave defined by Russell [22] as:

$$\frac{c_{Sol}}{\sqrt{gh}} = \sqrt{1 + \epsilon}, \tag{7}$$

the measured impulse wave celerities mainly scatter between 95% and 103% of the solitary wave celerity. This agrees with the findings by McFall and Fritz [23] and Evers et al. [24] for spatial impulse wave propagation in wave basins. The relative wave length L/h of Müller’s [7] experiments range between 9 and 56. According to Dean and Dalrymple [12], the generated waves cover the transition zone from intermediate-water ($2 < L/h \leq 20$) to shallow-water ($L/h > 20$). The measured wave celerities confirm this classification. In line with the additional text information in Müller [7], experiments no. 474, 589, 601, and 602 were not included in the analysis. The experiments featuring roughness elements at $\beta = 18.4^\circ$ (no. 562–588) were also not considered. All other experiments from Müller’s [7] appendix providing sufficient information on the impulse wave characteristics as well as the runup height were included in the analysis. The number of experiments included from Müller [7] is $n = 166$ (63 at $\beta = 18.4^\circ$, 17 at $\beta = 45^\circ$, 86 at $\beta = 90^\circ$).

The experiments by Hall and Watts [14] were conducted in a wave channel with a length of 25.9 m, a width of 4.3 m, and a depth of 1.2 m. The solitary waves were generated with a “pusher type” wave generator featuring a vertical pusher face mounted to a trolley, which was mechanically linked to a gravitationally accelerated drop weight. Both, wave height and runup height were optically measured. Besides slope angles $\beta = 10^\circ, 15^\circ, 25^\circ$, and 45° , also $\beta = 5^\circ$ was installed in the channel. However, the latter was not included into this analysis. The measured wave celerities c_{Sol} are within 88% to 94% of Equation (7) (Figure 2). Two experiments were not included into the analysis for this study as they were quite outside the trend of neighboring data points and therefore classified as obvious outliers ($R/h = 0.535$ and 0.679 , both at $\beta = 10^\circ$). The number of experiments included from Hall and Watts [14] is $n = 138$ (38 at $\beta = 10^\circ$, 37 at $\beta = 15^\circ$, 31 at $\beta = 25^\circ$, 32 at $\beta = 45^\circ$).

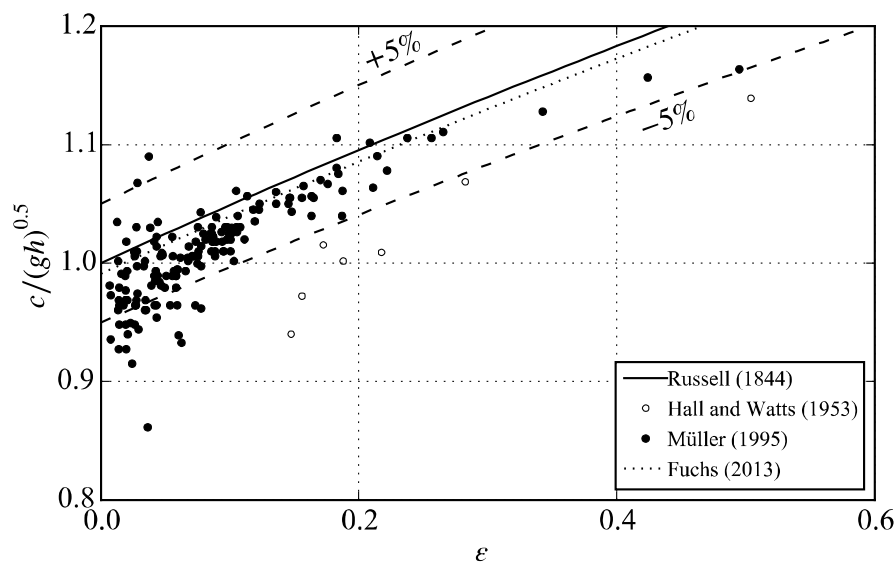


Figure 2. Relative wave crest celerity $c/(gh)^{0.5}$ versus relative wave amplitude ϵ from data sources from Müller [7], Hall and Watts [14], and Fuchs [20] and (—) solitary wave celerity (Equation (7)).

Fuchs [20] conducted experiments with a pneumatic piston-type wave generator in an 11 m long, 0.5 m wide, and 1 m deep channel. The inclinations of the runup slopes were set to $\tan \beta = 1/5, 1/2.5,$ and $1/1.5$; i.e., $\beta \approx 11.3^\circ, 21.8^\circ,$ and 33.7° . The solitary wave profiles were tracked with ultrasonic distance sensors and runup heights were measured optically. The measured wave celerities average out at 99.1% of Equation (7) (Figure 2). The number of experiments included from Fuchs [20] is $n = 19$ (7 at $\beta = 11.3^\circ, 6$ at $\beta = 22.8^\circ, 6$ at $\beta = 33.6^\circ$).

Street and Camfield [21] studied solitary wave reflection at a vertical wall, i.e., $\beta = 90^\circ$, in a 17 m long subsection of a channel with a length of 35 m and a width of 0.91 m. The piston-type wave generator was controlled with a hydraulic-servo-electronic system. Wave amplitudes were measured with capacitance wave gauges. Near shore deformation details were optically recorded. The runup data by Street and Camfield [21] was extracted with WebPlotDigitizer [25] from the original publication. The number of experiments included from Street and Camfield [21] is $n = 22$.

Maxworthy [19] studied solitary wave reflection at a vertical wall as well as head-on collision between two solitary waves in a 5 m long, 0.2 m wide, and 0.3 m deep channel. Only runup data at the wall was considered for this study. The waves were generated manually by pulling a plate through the channel. The wave characteristics and the runup height were measured optically. The runup data by Maxworthy [19] was extracted with WebPlotDigitizer [25] from the original publication. The number of experiments included from Maxworthy [19] is $n = 14$.

In total, 359 experiments were included into the analysis. The available information on wave celerities and lengths indicates that the waves contained in the dataset may be classified into the transition zone from intermediate-water to shallow-water or long waves, respectively. Figure 3a shows the runup height R over the wave amplitude a versus the slope parameter S_o introduced by Grilli et al. [26] with

$$S_o = 1.521 \frac{\tan \beta}{\sqrt{\epsilon}}, \tag{8}$$

for the overall dataset except for the experiments with $\beta = 90^\circ$. S_o allows for assessing whether a solitary wave is breaking or non-breaking during runup. Grilli et al. [26] stated $S_o > 0.37$ as the criterion for non-breaking solitary wave runup. As β approaches 90° , S_o tends to infinity. Therefore, experiments with $\beta = 90^\circ$ are not included in Figure 3. All other experiments satisfy $S_o \geq 0.37$. The experiment by Fuchs [20] with $S_o = 0.37$ (Figure 3), $\beta \approx 11.3^\circ$, and $\varepsilon = 0.69$ is shown in Figure 4 and features no distinct wave breaking characteristics. It is therefore assumed that the overall dataset consists of non-breaking wave runup. The limiting criterion $\varepsilon^{0.5} \gg 0.288 \tan\beta$ for Equation (5) stated by Synolakis [16] may be reformulated as $S_o \ll 5.28$ (Pujara et al. [10]) and is also included in Figure 3. Several experiments feature S_o values close to and larger than 5.28.

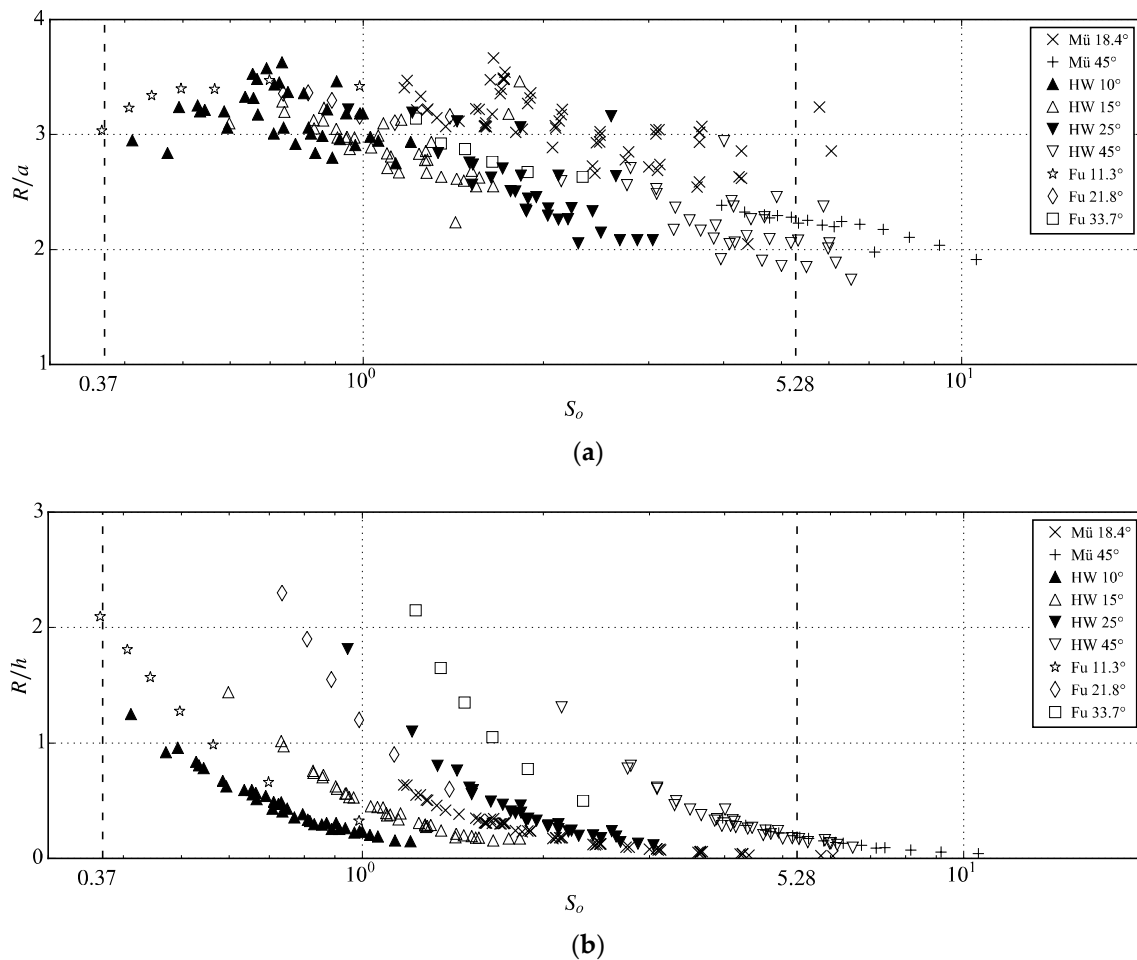


Figure 3. (a) Runup height over wave amplitude R/a and (b) runup height over stillwater depth R/h versus slope parameter S_o for experiments from data sources from Müller (Mü) [7] (without $\beta = 90^\circ$), Hall and Watts (HW) [14], and Fuchs (Fu) [20].

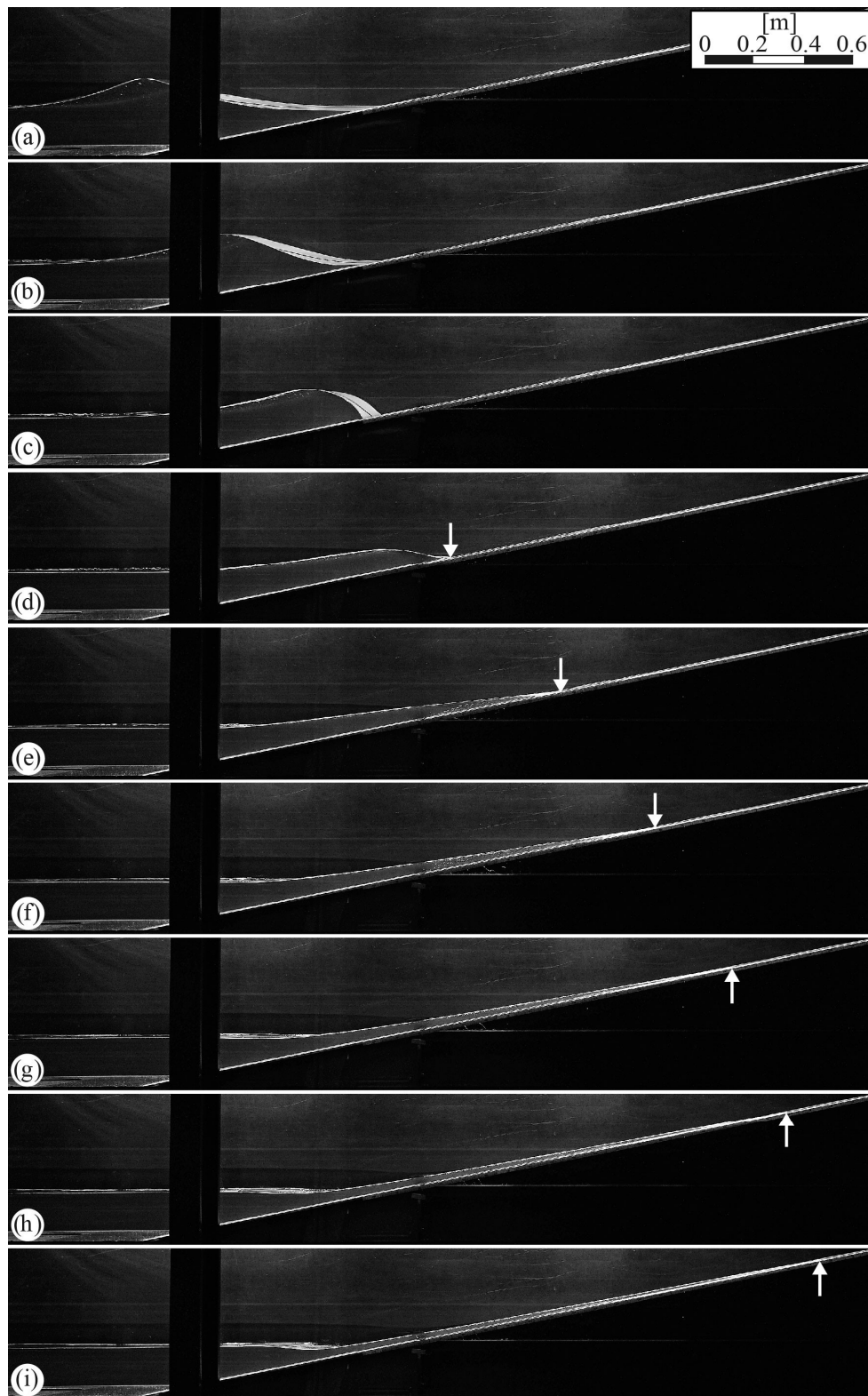


Figure 4. Solitary wave runup for $\tan\beta = 1/5.0$ ($\beta \approx 11.3^\circ$), $\varepsilon = 0.69$, and $S_0 = 0.37$, time increment between images $\Delta t = 0.2$ s, flow front indicated by arrow (reproduced from Fuchs [20]).

4. Results

4.1. Existing Prediction Equations

Equation (1) by Müller [7] predicts its underlying data well within a $\pm 20\%$ scatter range (Figure 5). Only few experiments with $\beta = 18.4^\circ$ exceed this range, i.e., the actually measured runup heights are more than 20% larger than the predicted values. Equation (2) was applied to get the effective wave length L_{Sol} to allow for the prediction of the solitary wave experiments by Hall and Watts [14], Fuchs [20], Street and Camfield [21], and Maxworthy [19]. However, these experiments are broadly underestimated and the measured runup heights are up to 70% higher than their prediction.

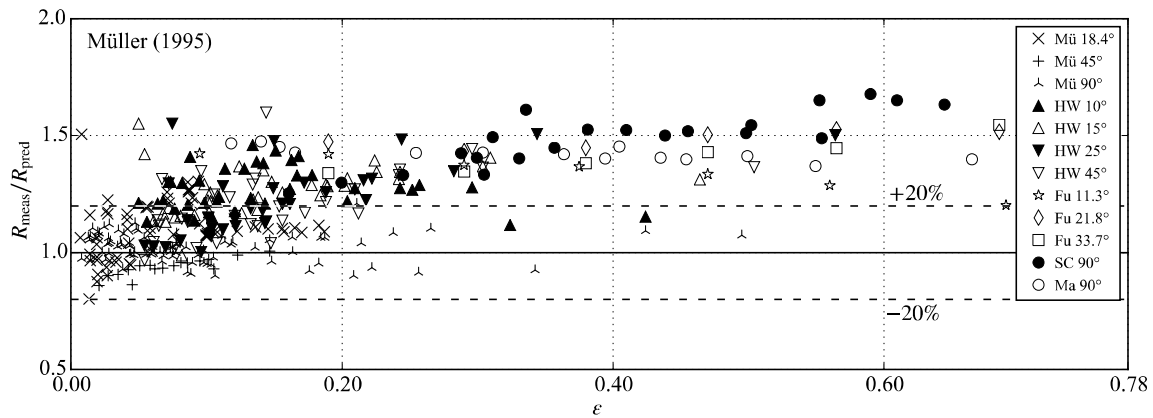


Figure 5. Measured over predicted (Equation (1) by Müller [7]) runup height R_{meas}/R_{pred} versus relative wave crest amplitude ϵ for experiments from data sources from Müller (Mü) [7], Hall and Watts (HW) [14], Fuchs (Fu) [20], Street and Camfield (SC) [21], and Maxworthy (Ma) [19].

The data by Hall and Watts [14] is predicted well within a $\pm 20\%$ scatter range by their empirically derived Equation (3) (Figure 6). Additionally, the runup experiments by Street and Camfield [21] and Maxworthy [19] with $\beta = 90^\circ$ are predicted within this range, although vertical walls were not considered by Hall and Watts [14]. For small relative wave amplitudes $\epsilon < 0.05$ to 0.1, the measured runup heights are up to 50% larger than the predicted values. Mainly the impulse wave data by Müller [7] is affected by this underestimation, as it features small ϵ . For $\epsilon > 0.1$, impulse wave runup is also well predicted.

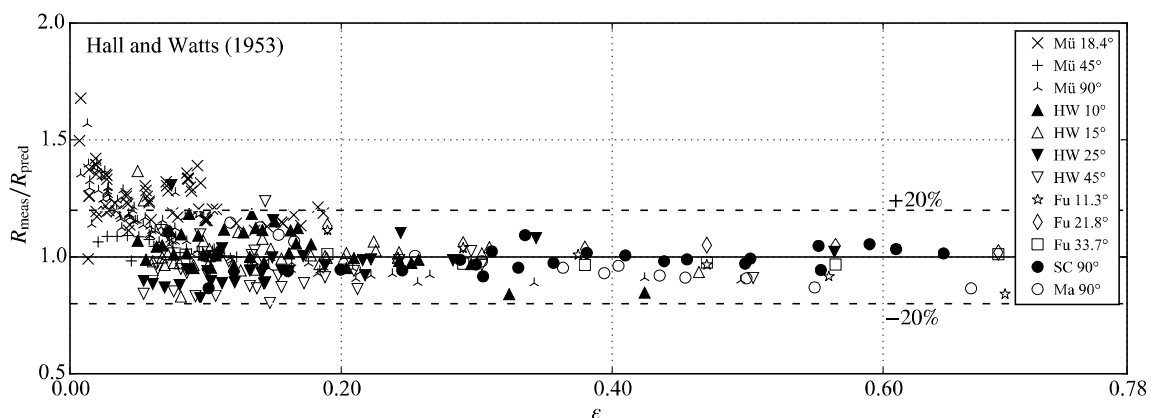


Figure 6. Measured over predicted (Equation (3) by Hall and Watts [14]) runup height R_{meas}/R_{pred} versus relative wave crest amplitude ϵ for experiments from data sources from Müller (Mü) [7], Hall and Watts (HW) [14], Fuchs (Fu) [20], Street and Camfield (SC) [21], and Maxworthy (Ma) [19].

Figure 7 excludes runup data at vertical walls, since Equation (4) by Fuchs and Hager [15] is not defined for $\beta = 90^\circ$. Equation (4) predicts its underlying data well. Additionally, the measured runup heights at $\beta = 10^\circ, 15^\circ,$ and 18.4° scatter within $\pm 20\%$ of the prediction. However, the runup data for $\beta = 25^\circ$ and 45° are predicted too conservatively for $\epsilon < 0.2$, i.e., the actual runup heights are up to 40% smaller than their predicted values.

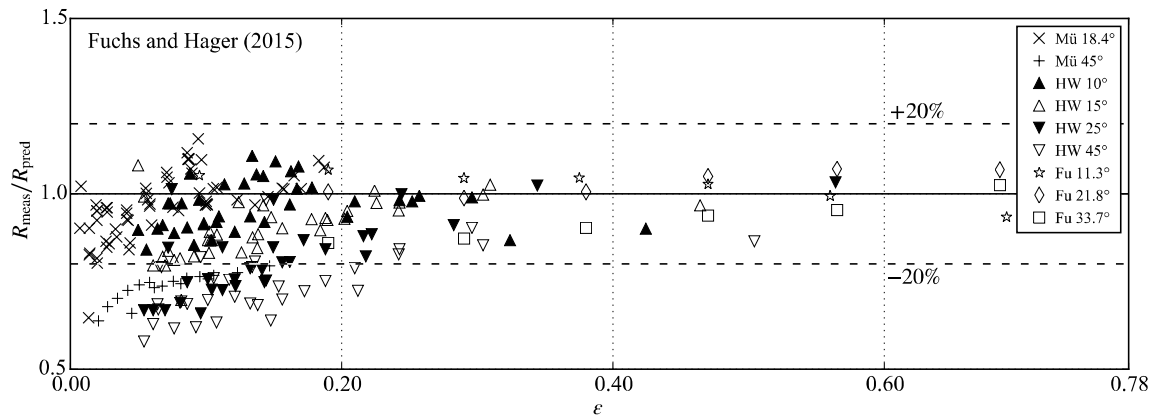


Figure 7. Measured over predicted (Equation (4) by Fuchs and Hager [15]) runup height R_{meas}/R_{pred} versus relative wave crest amplitude ϵ for experiments from data sources from Müller (Mü) [7] (without $\beta = 90^\circ$), Hall and Watts (HW) [14], and Fuchs (Fu) [20].

Equation (5) by Synolakis [16] yields runup heights equal to zero for $\beta = 90^\circ$. Therefore, these experiments are excluded from Figure 8. The measured values scatter broadly around the predicted runup heights both for solitary and impulse waves. While the measured runup heights for $\epsilon > 0.2$ are up to 50% smaller, the measurements for $\epsilon < 0.2$ are up to 100% above the prediction. The slope parameter S_0 of the latter experiments is close to 5.28, the upper limiting criterion of Equation (5).

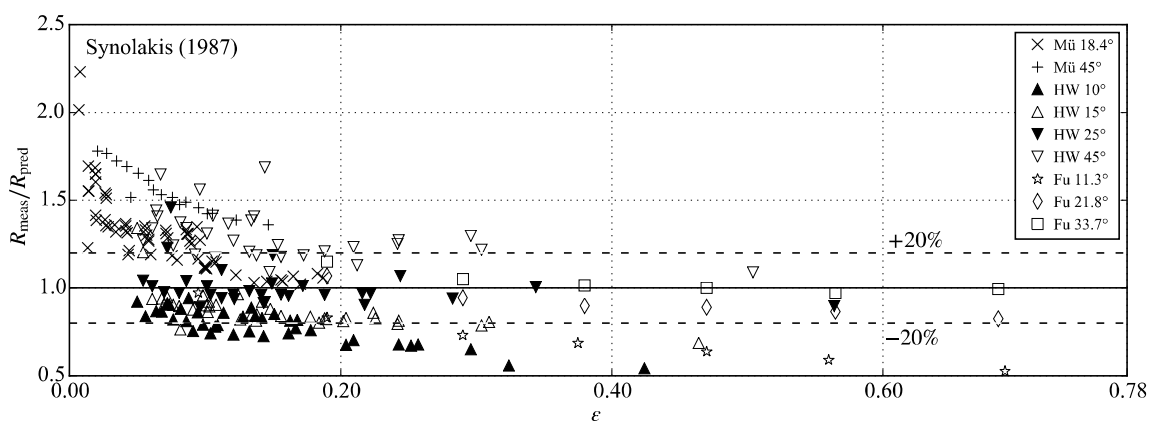


Figure 8. Measured over predicted (Equation (5) by Synolakis [16]) runup height R_{meas}/R_{pred} versus relative wave crest amplitude ϵ for experiments from data sources from Müller (Mü) [7] (without $\beta = 90^\circ$), Hall and Watts (HW) [14], and Fuchs (Fu) [20].

Equation (6) by Su and Mirie [17] was analytically derived for solitary wave runup at a vertical wall. Both impulse and solitary wave experiments with $\beta = 90^\circ$ scatter narrowly within $\pm 20\%$ around the prediction (Figure 9). There is no distinct effect of ϵ on the prediction quality, even for small ϵ . Also, the data with $\beta = 45^\circ$ scatter within this range. With decreasing slope angle β , the measured runup heights are more and more underestimated. For $\beta < 20^\circ$, the measurements are up to 80% larger than the predictions. However, this underestimation appears to be smaller for large ϵ .

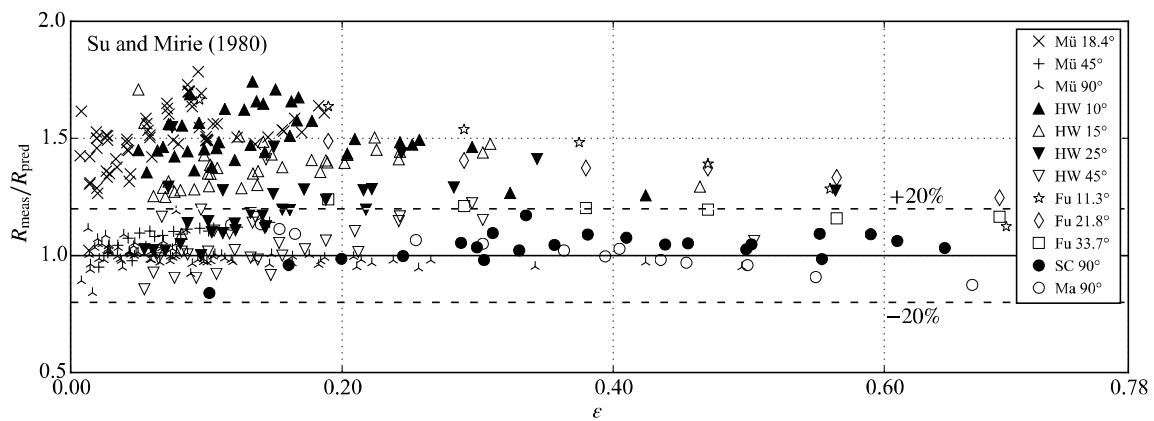


Figure 9. Measured over predicted (Equation (6) by Su and Mirie [17]) runup height $R_{\text{meas}}/R_{\text{pred}}$ versus relative wave crest amplitude ϵ for experiments from data sources from Müller (Mü) [7], Hall and Watts (HW) [14], Fuchs (Fu) [20], Street and Camfield (SC) [21], and Maxworthy (Ma) [19].

4.2. New Prediction Equation

Based on the findings in the previous sections, a new prediction approach is proposed. While Equation (1) by Müller [7] adequately captures the effect of the slope angle β from 18.4° to 90° , Equation (6) by Su and Mirie [17] yields good runup predictions at vertical walls for a broad range of wave amplitudes ϵ . In Figure 10, the runup heights of the overall experimental dataset are approximated ($R^2 = 0.98$) with:

$$\frac{R}{h} = \left(2\epsilon + \frac{1}{2}\epsilon^2 + \frac{3}{4}\epsilon^3 \right) \left(\frac{90^\circ}{\beta} \right)^{0.2}. \quad (9)$$

The first bracket includes Equation (6) by Su and Mirie [17] and the second bracket includes the effect of β from Equation (1) by Müller [7]. For $\beta = 90^\circ$ the latter term equals to 1 and for $\beta = 10^\circ$ it is approximately 1.55, i.e., the runup height increases with decreasing β . The measured runup heights scatter within circa $\pm 25\%$ of the prediction (Figure 10). The 2.5th and 97.5th percentile whiskers in Figure 11a show that more than 95% of the experiments are within a $\pm 20\%$ range. The maximum deviations of single experiments are within $\pm 30\%$. These experiments include $\epsilon < 0.2$ as well as large ϵ at comparatively gentle slope angles $\beta = 10^\circ$ and 11.3° . Figure 11b shows the direct comparison of the measured relative runup heights R_{meas}/h versus the predicted R_{pred}/h .

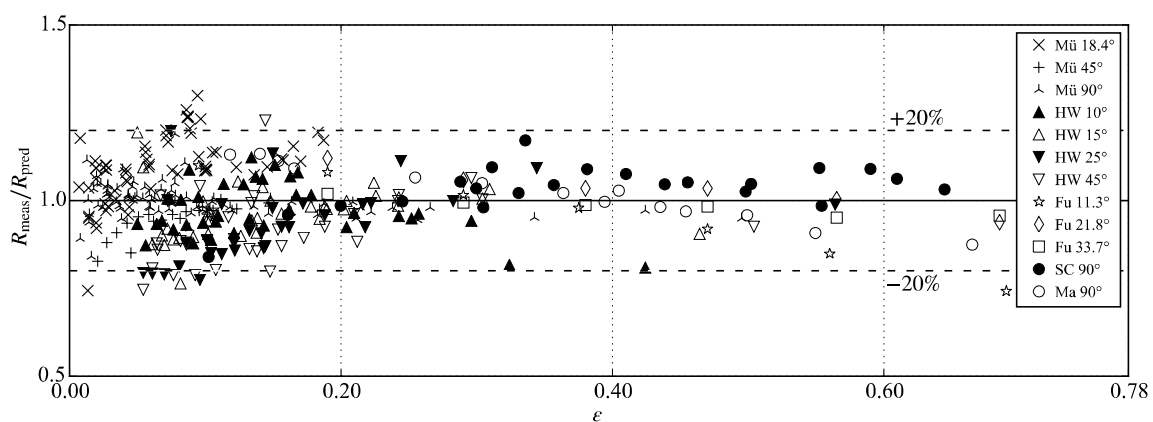


Figure 10. Measured over predicted (Equation (9)) runup height $R_{\text{meas}}/R_{\text{pred}}$ versus relative wave crest amplitude ϵ for experiments from data sources from Müller (Mü) [7], Hall and Watts (HW) [14], Fuchs (Fu) [20], Street and Camfield (SC) [21], and Maxworthy (Ma) [19].

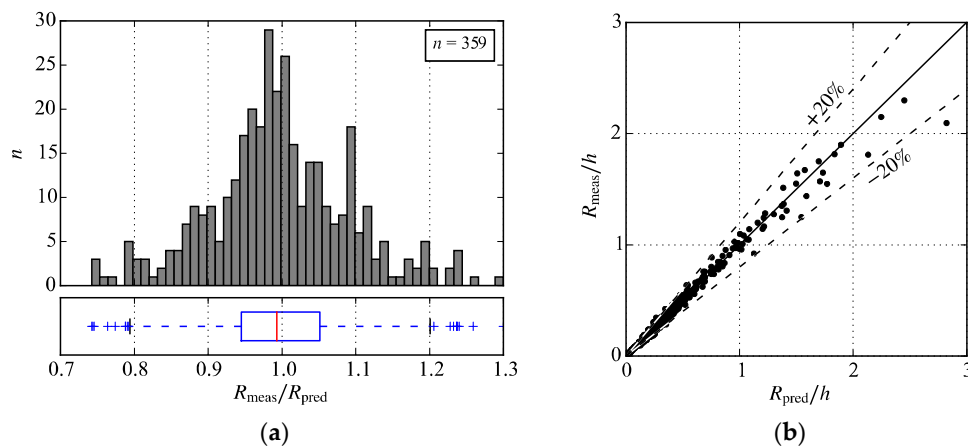


Figure 11. (a) Histogram and boxplot with whiskers at 2.5th and 97.5th percentile of measured over predicted (Equation (9)) runup heights R_{meas}/R_{pred} and (b) measured versus predicted runup heights R over stillwater depth h of the overall dataset.

As a simplified version of Equation (9), the following prediction equation for non-breaking impulse and solitary wave runup on steep to vertical slopes is proposed ($R^2 = 0.98$):

$$\frac{R}{h} = 2\epsilon e^{0.4\epsilon} \left(\frac{90^\circ}{\beta} \right)^{0.2} \quad (10)$$

The term $2\epsilon e^{0.4\epsilon}$ in Equation (10) approximates Su and Mirie’s [17] Equation (6) by multiplying the minimum runup height of 2ϵ for very small relative wave amplitudes ϵ with an exponential function accounting for the second- and third-order effects, which become significant for large ϵ . 33 additional experiments are added as a validation dataset to Figure 12, including data from Pedersen et al. [27] ($n = 5$; $\beta = 10^\circ$), Li and Raichlen [28] ($n = 22$; $\beta = 25.7^\circ$), and Losada et al. [29] ($n = 6$; $\beta = 45^\circ, 70^\circ, 90^\circ$; taken from Maiti and Sen [30]). The additional relative wave crest amplitudes ϵ range from 0.026 to 0.48. The scatter plot ($R^2 = 0.98$) of Equation (10) in Figure 12 is very similar to Figure 10 based on Equation (9). As shown in Figure 13a, the overall scatter is slightly shifted to the side of caution, i.e., overestimation, by this approximation therefore having a minor effect on the overall prediction quality. Figure 13b compares the approximation $2\epsilon e^{0.4\epsilon}$ with Equation (6). The deviations are around $\pm 2\%$ within the range of the analyzed dataset ($\epsilon \leq 0.69$) and -4% for a maximum $\epsilon = 0.78$ (McCowan [31]).

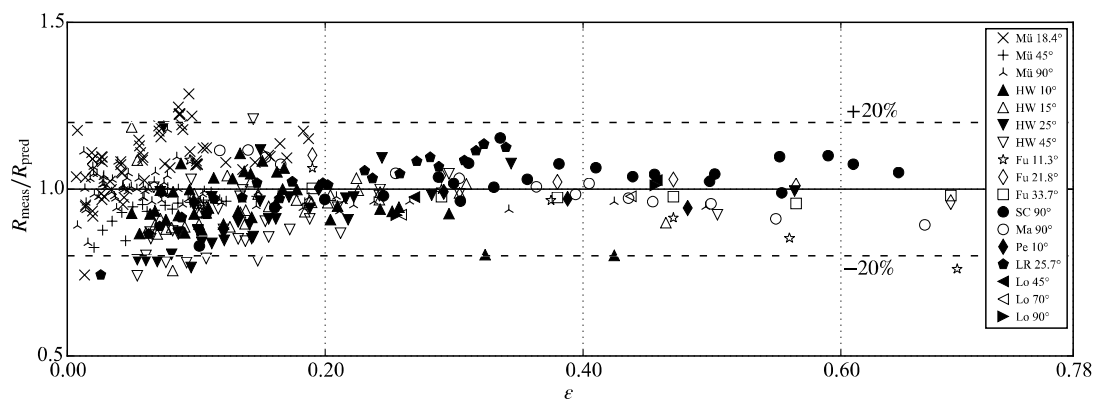


Figure 12. Measured over predicted (Equation (10)) runup height R_{meas}/R_{pred} versus relative wave crest amplitude ϵ for experiments from data sources from Müller (Mü) [7], Hall and Watts (HW) [14], Fuchs (Fu) [20], Street and Camfield (SC) [21], Maxworthy (Ma) [19], Pedersen et al. (Pe) [27], Li and Raichlen (LR) [28], and Losada et al. (Lo) [29].

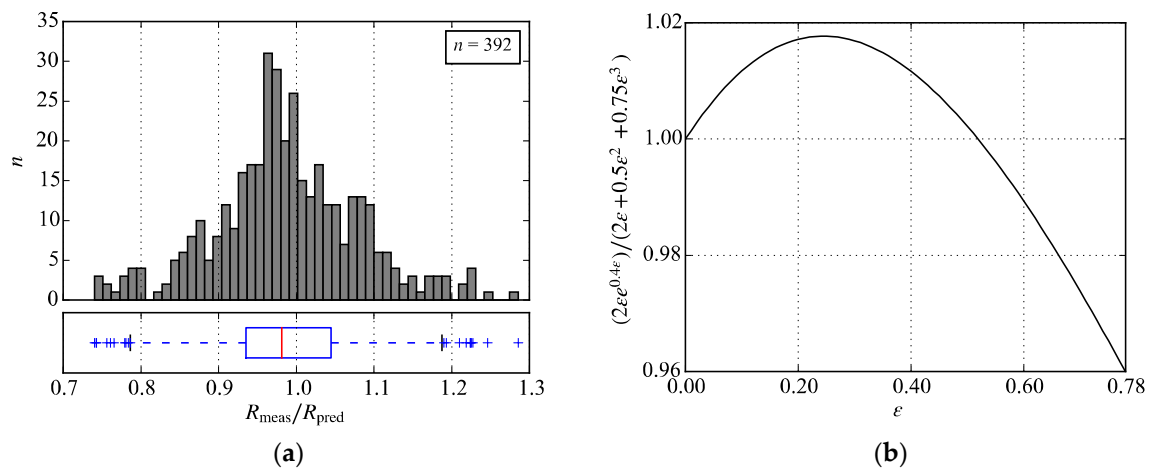


Figure 13. (a) Histogram and boxplot with whiskers at 2.5th and 97.5th percentile of measured over predicted (Equation (10)) runup height $R_{\text{meas}}/R_{\text{pred}}$ of the overall dataset; (b) $2\epsilon e^{0.4\epsilon}$ over Equation (6) versus relative wave amplitude ϵ .

5. Discussion

With $S_o \geq 0.37$, the overall dataset is assumed to include non-breaking wave runup. Considering a maximum relative wave crest amplitude $\epsilon = 0.78$ before runup according to McCowan [31], the minimum slope angle satisfying $S_o = 0.37$ is $\beta = 12^\circ$. For this study, also experiments with $\beta = 10^\circ$ and 11.3° were analyzed, which would lead to wave breaking for $\epsilon = 0.78$ according to S_o . Equation (10) tends to overestimate runup heights by large ϵ on these slopes (Figure 12). Therefore $S_o = 0.37$ is considered the lower application boundary of Equation (10) for β from 10° to 90° . Pujara et al. [10] proposed a more conservative breaking criterion $S_o \approx 0.4$ to 0.5 . With $S_o > 0.5$ to ensure no wave-breaking at $\beta = 10^\circ$, the maximum amplitude is $\epsilon \leq 0.3$, which still provides a useful range of application for less steep slopes.

Compared to Equation (1) by Müller [7], the new prediction Equation (10) contains solely the relative wave crest amplitude ϵ as the governing wave parameter instead of the wave height H and the wave length L . For the assessment of landslide generated impulse wave events, prediction equations are applied in sequence to cover a particular process chain, e.g., wave generation and runup (Bregoli et al. [8], McFall and Fritz [9]). In this context, the maximum relative scatter of a target value, e.g., R , is derived from the scatter of its individual input parameters, e.g., ϵ , H and/or L (Heller et al. [1]). While the scatter is not significantly altered by substituting H and L with ϵ for predicting Müller’s [7] measurements (Figures 5 and 12), the prediction uncertainty for the entire process chain may be reduced by including fewer parameters.

Fuchs and Hager [32] conducted scale family experiments of solitary wave runup and observed no significant scale effects for $h \geq 0.08$ m at $\beta = 11.3^\circ$. For their smallest investigated $\epsilon = 0.1$, this corresponds to a minimum runup height $R = 25$ mm. The dataset by Müller [7] contains six experiments at $\beta = 18.4^\circ$ with R between 12 and 24 mm induced by ϵ from 0.007 to 0.014. As shown in Figure 12, these experiments scatter around $\pm 20\%$ of the prediction. This range reflects the measurement accuracy as well as the experimental accuracy from repeatability tests (Müller [7]). As no distinct trend is observed in the data, scale effects are considered negligible. Also, the experiments by Maxworthy [19] feature $R < 25$ mm. However, these experiments were conducted at a much steeper slope with $\beta = 90^\circ$. In addition, the measured runup heights show no distinct deviation compared to the experiments by Street and Camfield [21], which were conducted at a three to four times larger scale (Figure 9).

The experimental setups considered in this study feature two-dimensional, plane, and smooth runup slopes, which represent a simplification of shorelines at prototype scale. Additional prototype

parameters include three-dimensional slope features, non-constant slopes, and rough surfaces. Strong curvatures along the shoreline cause flow diversion and concentration, respectively, which might lead to a significant over- or underestimation of the actual runup height. Therefore, Equation (10) should only be applied to evenly formed slope bathymetries and topographies. Non-constant slopes complicate the determination of a single slope angle β . A sensitivity analysis allows for assessing the influence of β for the slope range derived from field data. The term of Equation (10) including the slope angle β yields larger runup heights for decreasing β . A decrease from 90° to 45° leads to an increase in runup height of 15%. A decrease from 20° to 10° also leads to an increase of 15%. Therefore, the effect of β is stronger for lower slope angles. Teng et al. [33] conducted experiments on solitary wave runup on both smooth and rough slopes. The roughness effect was found to be negligible on relatively steep slopes ($\beta \geq 20^\circ$), while it reduced the measured runup heights by up to approximately 30% for $\beta = 15^\circ$ and by 50% for $\beta = 10^\circ$. However, runup height estimation based on Equation (10), which is derived from experiments featuring smooth slopes, would err on the side of caution. Finally, the scatter range of $\pm 20\%$ needs to be taken into account as a safety margin for runup height predictions at prototype scale.

6. Conclusions

The runup height of impulse waves as well as solitary waves on slope angles between 10° and 90° was analyzed. While a solitary wave features a single wave crest without a following trough, an impulse wave train consists of multiple wave crests and troughs. A dataset with $n = 359$ experiments was compiled from literature including runup heights by both wave types. Regarding impulse wave runup, the first wave within the wave train was analyzed based on the experiments by Müller [7]. The overall dataset was compared with both empirical and analytical equations from literature, and a new semi-empirical prediction equation was presented. Additionally, $n = 33$ experiments were included as a validation dataset. The main findings are:

- Solitary waves are a suitable proxy for modelling the runup height of the first wave within an impulse wave train;
- Commonly applied prediction equations may significantly underestimate the measured runup heights by small relative wave crest amplitudes $\varepsilon < 0.1$;
- A new equation for non-breaking impulse wave runup on slope angles from 10° to 90° predicts the overall dataset within a $\pm 20\%$ scatter for ε between 0.007 and 0.69 as the single wave input parameter.

Author Contributions: Data analysis, F.M.E.; writing—original draft preparation and editing, F.M.E.; writing—review, R.M.B.; funding acquisition, R.M.B.

Funding: This work was funded by the Swiss Federal Office of Energy SFOE / Bundesamt für Energie BFE (Project No. SI/501802-01) and is part of the Swiss Competence Center for Energy Research—Supply of Electricity (SCCER-SoE).

Acknowledgments: The authors would like to thank the experimenters for publishing their data in a way allowing for reuse. Willi H. Hager is acknowledged for helpful discussions. Figure 4 was provided by courtesy of Helge Fuchs.

Conflicts of Interest: The authors declare no conflict of interest.

Nomenclature

Symbol	Term	Unit
a	Wave crest amplitude	[m]
c	Wave crest celerity	[m/s]
c_{Sol}	Solitary wave crest celerity	[m/s]
h	Stillwater depth	[m]

H	Wave height	[m]
g	Gravitational acceleration	[m/s ²]
L	Wave length	[m]
L_{Sol}	Solitary wave length	[m]
n	Number of experiments	[-]
R	Runup height	[m]
R^2	Coefficient of determination	[-]
S_0	Slope parameter	[-]
β	Slope angle	[°]
ε	Relative wave crest amplitude	[-]
Fu	Fuchs [20]	
HW	Hall and Watts [14]	
Li	Li and Raichlen [28]	
Lo	Losada et al. [29]	
Ma	Maxworthy [19]	
Mü	Müller [7]	
Pe	Pedersen et al. [27]	
SC	Street and Camfield [21]	

References

- Heller, V.; Hager, W.H.; Minor, H.-E. Landslide generated impulse waves in reservoirs: Basics and computation. In *VAW-Mitteilung 211*; Boes, R., Ed.; ETH Zurich: Zürich, Switzerland, 2009.
- Roberts, N.J.; McKillop, R.; Hermanns, R.L.; Clague, J.J.; Oppikofer, T. Preliminary global catalogue of displacement waves from subaerial landslides. In *Landslide Science for a Safer Geoenvironment*; Sassa, K., Canuti, P., Yin, Y., Eds.; Springer: Cham, Switzerland, 2014; Volume 3, pp. 687–692. ISBN 978-3-319-04996-0.
- Miller, D.J. *Giant Waves in Lituya Bay, Alaska*; Geological Survey Professional Paper No. 354-C; U.S. Government Printing Office: Washington, DC, USA, 1960.
- Roberts, N.J.; McKillop, R.J.; Lawrence, M.S.; Psutka, J.F.; Clague, J.J.; Brideau, M.-A.; Ward, B.C. Impacts of the 2007 landslide-generated tsunami in Chehalis Lake, Canada. In *Landslide Science and Practice*; Margottini, C., Canuti, P., Sassa, K., Eds.; Springer: Berlin/Heidelberg, Germany, 2013; Volume 6, pp. 133–140. ISBN 978-3-642-31319-6.
- Higman, B.; Shugar, D.H.; Stark, C.P.; Ekström, G.; Koppes, M.N.; Lynett, P.; Dufresne, A.; Haeussler, P.J.; Geertsema, M.; Gulick, S.; et al. The 2015 landslide and tsunami in Taan Fiord, Alaska. *Sci. Rep. UK* **2018**, *8*, 12993. [[CrossRef](#)]
- Fuchs, H.; Boes, R. Berechnung felsrutschinduzierter Impulswellen im Vierwaldstättersee. *Wasser Energ. Luft* **2010**, *102*, 215–221. (In German) [[CrossRef](#)]
- Müller, D.R. Auflaufen und Überschwappen von Impulswellen an Talsperren. In *VAW-Mitteilung 137*; Vischer, D., Ed.; ETH Zurich: Zürich, Switzerland, 1995. (In German)
- Bregoli, F.; Bateman, A.; Medina, V. Tsunamis generated by fast granular landslides: 3D experiments and empirical predictors. *J. Hydraul. Res.* **2017**, *55*, 743–758. [[CrossRef](#)]
- McFall, B.C.; Fritz, H.M. Runup of granular landslide-generated tsunamis on planar coasts and conical islands. *J. Geophys. Res. Oceans* **2017**, *122*, 6901–6922. [[CrossRef](#)]
- Pujara, N.; Liu, P.L.-F.; Yeh, H. The swash of solitary waves on a plane beach: Flow evolution, bed shear stress and run-up. *J. Fluid Mech.* **2015**, *779*, 556–597. [[CrossRef](#)]
- Hafsteinsson, H.J.; Evers, F.M.; Hager, W.H. Solitary wave run-up: Wave breaking and bore propagation. *J. Hydraul. Res.* **2017**, *55*, 787–798. [[CrossRef](#)]
- Dean, R.G.; Dalrymple, R.A. *Water Wave Mechanics for Engineers and Scientists*; World Scientific Publishing: Singapore, 1991.
- Lo, H.-Y.; Park, Y.S.; Liu, P.L.-F. On the run-up and back-wash processes of single and double solitary waves—An experimental study. *Coast. Eng.* **2013**, *80*, 1–14. [[CrossRef](#)]

14. Hall, J.V.; Watts, G.M. *Laboratory Investigation of the Vertical Rise of Solitary Wave on Impermeable Slopes*; Technical Memo Report No. 33; U.S. Army Corps of Engineers, Beach Erosion Board: Washington, DC, USA, 1953.
15. Fuchs, H.; Hager, W.H. Solitary impulse wave transformation to overland flow. *J. Waterw. Port C ASCE* **2015**, *141*, 04015004. [[CrossRef](#)]
16. Synolakis, C.E. The runup of solitary waves. *J. Fluid Mech.* **1987**, *185*, 523–545. [[CrossRef](#)]
17. Su, C.H.; Mirie, R.M. On head-on collisions between two solitary waves. *J. Fluid Mech.* **1980**, *98*, 509–525. [[CrossRef](#)]
18. Cooker, M.J.; Weidman, P.D.; Bale, D.S. Reflection of a high-amplitude solitary wave at a vertical wall. *J. Fluid Mech.* **1997**, *342*, 141–158. [[CrossRef](#)]
19. Maxworthy, T. Experiments on collisions between solitary waves. *J. Fluid Mech.* **1976**, *76*, 177–186. [[CrossRef](#)]
20. Fuchs, H. Solitary impulse wave run-up and overland flow. In *VAW-Mitteilung 221*; Boes, R., Ed.; ETH Zurich: Zürich, Switzerland, 2013.
21. Street, R.L.; Camfield, F.E. Observations and experiments on solitary wave deformation. In Proceedings of the 10th International Conference on Coastal Engineering, Tokyo, Japan, September 1966; ASCE: Reston, VA, USA, 1966. [[CrossRef](#)]
22. Russell, J.S. *Report on Waves*; Report of the 14th Meeting of the British Association for the Advancement of Science; British Association: York, UK, 1944; pp. 311–390.
23. McFall, B.C.; Fritz, H.M. Physical modelling of tsunamis generated by three-dimensional deformable granular landslides on planar and conical island slopes. *Proc. R. Soc. A Math. Phys.* **2016**, *472*, 20160052. [[CrossRef](#)] [[PubMed](#)]
24. Evers, F.M.; Hager, W.H.; Boes, R.M. Spatial impulse wave generation and propagation. *J. Waterw. Port C ASCE* **2019**, in press. [[CrossRef](#)]
25. Rohatgi, A.; Rehberg, S.; Stanojevic, Z. ankitrohatgi/WebPlotDigitizer: Version 4.1 of WebPlotDigitizer (Version v4.1). *Zenodo* **2018**. [[CrossRef](#)]
26. Grilli, S.T.; Svendsen, I.A.; Subramanya, R. Breaking criterion and characteristics for solitary waves on slopes. *J. Waterw. Port C ASCE* **1997**, *123*, 102–112. [[CrossRef](#)]
27. Pedersen, G.K.; Lindstrøm, E.; Bertelsen, A.F.; Jensen, A.; Laskovski, D.; Sælevik, G. Runup and boundary layers on sloping beaches. *Phys. Fluids* **2013**, *25*, 012102. [[CrossRef](#)]
28. Li, Y.; Raichlen, F. Solitary wave runup on plane slopes. *J. Waterw. Port C ASCE* **2001**, *127*, 33–44. [[CrossRef](#)]
29. Losada, M.A.; Vidal, C.; Nunez, J. *Sobre El Comportamiento de Ondas Propagándose por Perfiles de Playa en Barra y Diques Sumergidos*; Dirección General de Puertos y Costas Programa de Clima Marítimo; Universidad de Cantabria: Cantabria, Spain, 1986. Publicación No. 16. (In Spanish)
30. Maiti, S.; Sen, D. Computation of solitary waves during propagation and runup on a slope. *Ocean Eng.* **1999**, *26*, 1063–1083. [[CrossRef](#)]
31. McCowan, J. On the highest wave of permanent type. *Lond. Edinb. Dublin Philos. Mag. J. Sci.* **1894**, *38*, 351–358. [[CrossRef](#)]
32. Fuchs, H.; Hager, W.H. Scale effects of impulse wave run-up and run-over. *J. Waterw. Port C ASCE* **2013**, *138*, 303–311. [[CrossRef](#)]
33. Teng, M.H.; Feng, K.; Liao, T.I. Experimental study on long wave run-up on plane beaches. In Proceedings of the 10th International Offshore and Polar Engineering Conference, Seattle, WA, USA, 28 May–2 June 2000; The International Society of Offshore and Polar Engineers, ISOPE-I-00-310. pp. 660–664.

